Int. J. Electrochem. Sci., 14 **(2019)** 6276 – 6282, doi: 10.20964/2019.07.72

International Journal of
ELECTROCHEMICAL
SCIENCE
www.electrochemsci.org

Short Communication

Shape-controlled Co_3O_4 as Advanced Electrode Materials for High-Performance Supercapacitor

Song Zhao[*], *Zhongbin Wei*

Department of mechanical and electrical technology, Xijing University, Xi'an 710123, China
[*]E-mail: zhaosongxj@sina.com

Received: 3 April 2019 / *Accepted:* 5 May 2019 / *Published:* 10 June 2019

Long-term cycle performance is a key factor for the supercapacitors that used pseudocapacitive materials. It is known to all that the morphology structures have direct influences on the electrochemical performance of the supercapacitors. In this work, shape-controlled Co_3O_4 electrode materials are successfully prepared and used as electrode materials for the supercapacitors. The different morphologies are Co_3O_4 nano-spheres and Co_3O_4 nano-rods, respectively. Among these two Co_3O_4 electrode materials, the Co_3O_4 nano-spheres shows more excellent electrochemical performance, with 96% capacity retention after 5000 cycles at the high current density of 5 A g^{-1}.

Keywords: Co_3O_4, nano-spheres, nano-rods, supercapacitors, capacity, electric vehicle

1. INTRODUCTION

With the increasing demands for the energy, the current fossil fuel could not satisfy the need for the people all over the world [1]. During the past decades, the researchers have always devoted themselves into finding new energy storage systems. Supercapacitors are one of the most promising candidates for the next generation energy storage system due to their high power density and fast recharge ability [2, 3]. So far, many works about the employment of electrode materials for the supercapacitors have been reported in the literatures [4, 5, 6]. Among various electrode materials for the supercapacitors, Co_3O_4-based electrodes are the most excellent for the reported supercapacitors [7, 8, 9].

Recently, some works about Co_3O_4 materials for the supercapacitors have figured out the Co_3O_4 materials have some disadvantages as the electrode materials [10, 11]. Li et al used manganese doped Co_3O_4 mesoporous nano-needle as the electrode materials for the supercapacitors [12]. The as-prepared COMN shows excellent electrochemical performance. This nanostructure is beneficial for the short ion diffusion path [13]. As a result, the supercapacitors display high rate performance and high

energy density. However, there are no works about controlling the morphology of the Co_3O_4 to improve the cycle stability of the supercapacitors [14, 15].

In our work, shape-controlled Co_3O_4 electrode materials are successfully prepared and used as electrode materials for the supercapacitors. The different morphologies are Co_3O_4 nano-spheres and Co_3O_4 nano-rods, respectively. Among these two Co_3O_4 electrode materials, the Co_3O_4 nano-spheres shows more excellent electrochemical performance, with 96% capacity retention after 5000 cycles at the high current density of 5 A g^{-1}. This superior electrochemical performance may be ascribed to the unique structure of Co_3O_4 nano-spheres, which could provide accessible ion diffusion pathway for the redox reaction.

2. EXPERIMENTAL

2.1. Preparation of various morphologies of Co_3O_4

Hydrothermal reaction was used to synthesis nanostructured Co_3O_4. Typically, 0.593 g $Co(NO_3)_2 \cdot 6H_2O$ and 0.605 g $CO(NH_2)_2$ were dissolved in 60 mL de-ionized water, and stirred for 30 min. Then, the obtained solution was transferred and sealed in an 80 mL Teflon-lined autoclave, and kept at 110℃ for 10h and 24h, respectively. After cooling down to the room temperature, the reactant was washed by den-ionized water and alcohol, and dried at 60℃. Finally, the product was heated in air at 400℃ for 2 h to obtain nanostructured Co_3O_4 and named as CO-NS and CO-NR, respectively.

2.2. Materials Characterization

The as-obtained samples were characterized by using a scanning electron microscope (SEM, JSM-7001F), an X-ray diffractometer (XRD, D8 Advance, BRUKER). X-ray photoelectron spectroscopy (XPS) was performed on a Thermo ESCALAB 250Xi in an ultra-high vacuum set-up equipped with an Al Kα X-ray source.

2.3. Electrochemical Measurements

The working electrode was prepared by coating the slurry of the active material (20 mg), carbon black (2.5 mg), and 60wt% polytetrafluoroethylene (1.6 mL) in small amount of ethanol on Ni foam substrate. Subsequently, the electrodes were dried at 110℃ for 24 h. Electrochemical measurements were conducted on an electrochemical working station (CHI 660E). All electrochemical behaviors of the working electrodes were cyclic voltammetry, galvanostatic charge-discharge and cycling stability.

3. RESULTS AND DISCUSSION

Figure 1 displays the SEM images of the as-prepared various morphologies of Co_3O_4 materials.

As shown in Figure 1a and b, the Co_3O_4 shows nano-spheres (CO-NS) structure. The dimeter of the Co_3O_4 nao-spheres is about 200-280 nm. With the increase of the pixel, it can be seen clearly that the surface of the Co_3O_4 nano-sphere is consisted of many nano-sheets [16,17]. This structure is beneficial for the restore of the electrolyte. Besides, it provides short path way for the transport of the ions. As for the Figure 1c and d, the Co_3O_4 exhibits nano-rods (CO-NR) structure. It can be seen that the CO-NR is uniformly dispersed in the SEM image, indicating the homogeneity of the Co_3O_4.

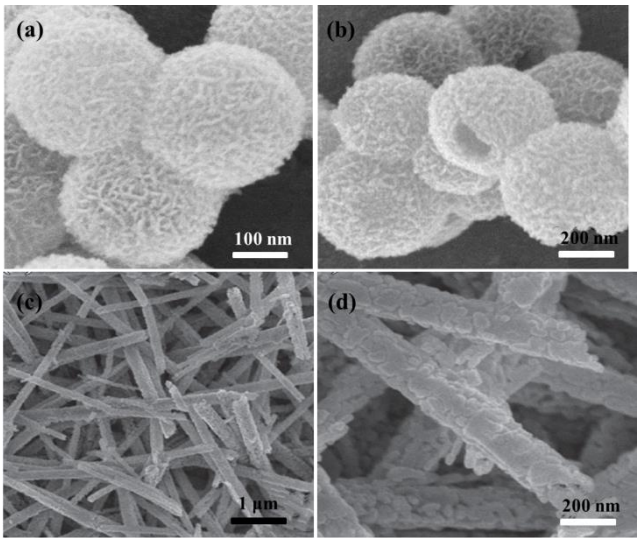

Figure 1. (a), (b) SEM images of the Co_3O_4 nano-spheres, (c), (d) SEM images of Co_3O_4 nano-rods.

To prove the successful preparation of the CO-NS and CO-NR, XRD test was conducted for the samples at the 2 theta from 10° to 80°. As shown in Figure 2, the as-prepare CO-NS and CO-NR show typical diffraction peaks of the Co_3O_4, indicating the purity of the as-prepared Co_3O_4 materials. All of the diffraction peaks are well matched with the standard card of Co_3O_4 [18]. Therefore, from the XRD results, it can be proved that the CO-NS and CO-NR are successfully prepared. The high purity of the Co_3O_4 electrode materials is significant important for the electrochemical performance of the supercapacitors.

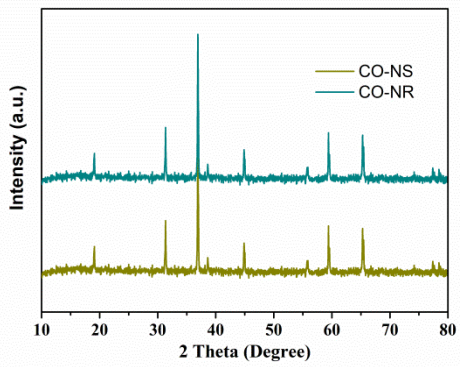

Figure 2. XRD pattern of the Co_3O_4 nano-spheres and Co_3O_4 nano-rods.

To further confirm the presence of the Co element in the CO-NS, the XPS spectrum for the CO-NS is tested. As shown in Figure 3, in the Co 2p XPS spectrum, there are two strong peaks at 780.6 and 796.1 eV, respectively. They represent the Co $2p_{3/2}$ and Co $2p_{1/2}$ spin–orbit peaks, respectively [19]. Meanwhile, two peaks at 785.9 and 801.4 eV are corresponding to the shake-up satellite peaks in the CO-NS materials, demonstrating the characteristic of Co_3O_4 phase. Moreover, the peaks at 779.8 and 795.2 eV are fitted with Co^{3+} [20]. The two peaks at 781.1 and 796.4 eV are assigned to Co^{2+}. In all, the XPS test could confirm the successful preparation of the Co_3O_4 based electrode materials for the supercapacitors. Besides, this result is consistent with the XRD results. They prove the preparation of the various morphologies of the Co_3O_4 electrode materials.

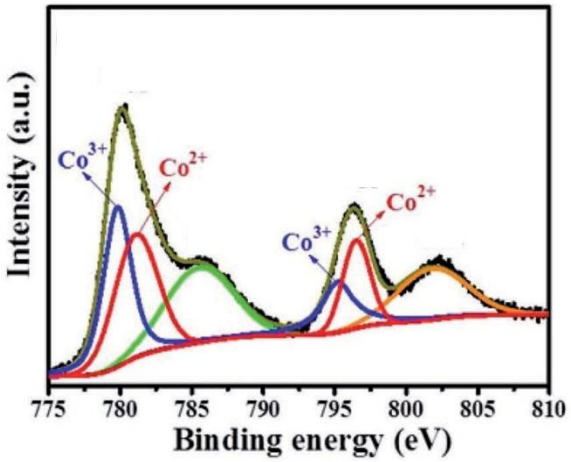

Figure 3. The XPS spectrum of Co 2p for the CO-NS.

Figure 4a shows the DC curves of the CO-NS at various current densities from 1 A g^{-1} to 20 A g^{-1}. The DC measurements are conducted with a voltage window of 0- 0.45 V. The capacities of the CO-NS are 686, 620, 536, 521, 435 F g^{-1} at the current density of 1, 2, 5, 10 and 20 A g^{-1}, respectively. Figure 4c is the DC curves of the as-prepared CO-CR. It could be clearly observed that the CO-NR shows smaller capacity value than CO-NS. Besides, the discharge and charge time of the CO-NR is shorter than the CO-NS. Therefore, the CO-NS exhibits higher capacity value as the electrode materials for the supercapacitors. As shown in Figure 4c, the specific capacities of the CO-NR electrode are 610, 519, 326, 121 and 35 F g^{-1} at the current density of 1, 2, 5, 10 and 20 A g^{-1}. From this, it can be clearly obtained that the CO-NS electrode materials could endure various current densities without severe capacity fading. However, for the CO-NR electrode, it suffers from obvious capacity fading during the increase of the current densities. This results prove that the morphology of the as-prepared Co_3O_4 electrode materials have great influence on the electrochemical performance of the supercapacitors.

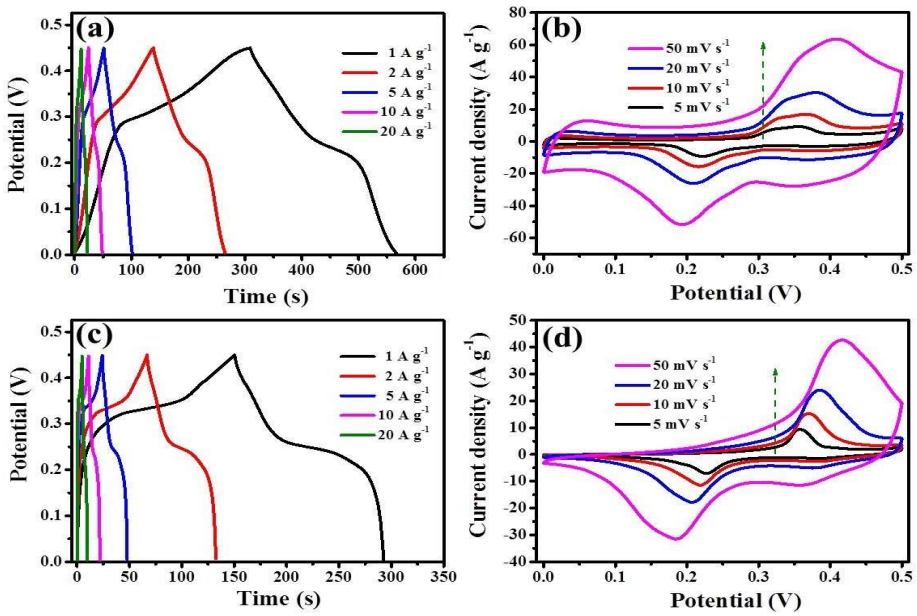

Figure 4. (a), (c) The DC profiles of the CO-NS and CO-NR electrode at various current densities from 1 A g^{-1} to 20 A g^{-1}. (b) (d) The CV curves of the CO-NS and CO-NR electrode.

Figure 4b demonstrates the CV profiles of the CO-NS with various scan rates between 0 and 0.5 V. The CO-NS displays two redox peaks at 0.23 V and 0.35 V at the scan rate of 5 mV s^{-1}. This indicates that the capacity value of CO-NS electrode is mainly controlled by the redox reaction of Co^{2+}/Co^{3+}. With the increase of the scan rate from 5 to 50 mV s^{-1}, the peak value of anode peak gradually turns to 0.4 V. However, the cathode peak value turns to 0.18 V. As for the movement of the cathode and anode peaks, it is ascribed to the redox reaction which is determined by the charge transfer dynamics. In a word, the CV curves of the CO-NS show perfect stable electrochemical performance. As shown in Figure 4d, in terms of the CV curves of the CO-NR, it can be seen that it exhibits bad cycle stability with the increase of the scan rate from 5 to 50 mV s^{-1}. This indicates that the capacities of the CO-NR electrode fade rapidly with the increase of the current densities from 5 to 50 mV s^{-1}. This phenomenon is according with the discharge/charge profiles of the CO-NR electrode (Figure 4c).

From above electrochemical results, it can be seen that the CO-NS electrode has more excellent electrochemical performance than the CO-NR electrode. Therefore, the long-term cycle performance of the CO-NS electrode was tested at the high current density of 5 A g^{-1} for 5000 cycles. As shown in Figure 5, the CO-NS electrode shows 96% capacity retention after 5000 cycles at the current density of 5 A g^{-1}. This is mainly due to the perfect structure of CO-NS, which could provide accessible ion diffusion pathway for the redox reaction. Besides, this structure is beneficial for the transport of the electronics. As a result, the electronic conductivity is greatly improved by using CO-NS electrode. In all, due to the perfect structure of the CO-NS, the CO-NS electrode materials exhibit superior cycle stability and high specific capacities even at the high current densities.

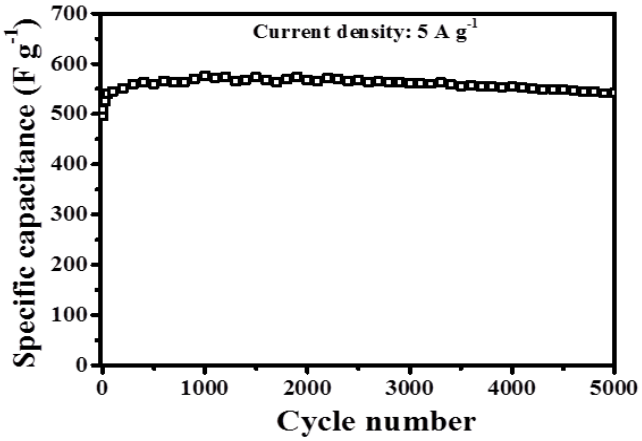

Figure 5. The long-term cycle performance of CO-NS for 5000 cycles.

Table 1 shows the electrochemical performance of the various electrode materials for the supercapacitors. It can be seen that the as-prepared CO-NS electrodes exhibit superior cycle stability. The CO-NS electrode shows 96% capacity retention after 5000 cycles at the current density of 5 A g^{-1}. This excellent electrochemical performance is ascribed to the perfect structure of the electrode, which could have ability to transport ions in the electrolyte. Therefore, this work may provide a promising way to prepared electrode materials for the supercapacitors.

Table 1. Comparison of the CO-NS with other reported electrode materials for the supercapacitors.

Electrode	Current Density	Capacity Retention	Ref
GPC	10 A g^{-1}	81% (1000 cycles)	21
CO-nanosheets	1 A g^{-1}	93% (5000 cycles)	22
CoO@Co_3O_4	3 A g^{-1}	74% (5000 cycles)	23
CO-NS	5 A g^{-1}	96% (5000 cycles)	This Work

4. CONCLUSIONS

In summary, the shape-controlled Co_3O_4 electrode materials are successfully prepared and used as electrode materials for the supercapacitors. The different morphologies are Co_3O_4 nano-spheres and Co_3O_4 nano-rods, respectively. Among these two Co_3O_4 electrode materials, the Co_3O_4 nano-spheres shows more excellent electrochemical performance, with 96% capacity retention after 5000 cycles at the high current density of 5 A g^{-1}. This superior electrochemical performance may be ascribed to the unique structure of Co_3O_4 nano-spheres, which could provide accessible ion diffusion pathway for the redox reaction.

ACKNOWLEDGEMENT
We thank the financial support from the Xijing University.

References

1. J. X. Zhang, Z. Z. Zhang, Y. T. Jiao, H. X. Yang, Y. Q. Li, J. Zhang and P. Gao, *J. Power Sources*, 419 (2019) 99.
2. Y. J. Zhou, C. Y. Liu, X. Li, L. L. Sun, D. Y. Wu, J. Z. Li, P. W. Huo and H. Q. Wang, *J. Alloy Compud*., 790 (2019) 36.
3. Z. Tian, J. H. Yin, X. M. Wang and Y. Z. Wang, *J. Alloy Compud*., 777 (2019) 806.
4. N. Wang, W. Dou, S. F. Hao, Y. Cheng, D. Zhou, X. M. Huang, C. Jiang and X. Cao, *Nano Energ*., 56 (2019) 868-874.
5. J. W. Li, X. F. Li, D. B. Xiong, L. Z. Wang and D. J. Li, *Appl. Surf. Sci*., 475 (2019) 285.
6. Y. F. Gao, Y. C. Xia, H. J. Wan, X. Xu and S. Jiang, *Electrochim. Acta*, 301 (2019) 294.
7. L. K. Que, L. Zhang, C. Wu, Y. Zhang, C. H. Pei and F. D. Nie, *Carbon*, 145 (2019) 281.
8. G. M. Li, M. Z. Chen, Y. O. Yang, D. Yao, L. Lei, L. Wang, X. F. Xia, W. Lei, S. M. Chen, Q. L. Hao, *Appl. Surf. Sci*., 469 (2019) 941.
9. L. X. Han, Z. F. Xu, J. Wu, X. Q. Guo, H. L. Zhu, H. Z. Cui, *J. Alloy Compud*., 729 (2017) 1183.
10. Z. J. Shi, L. Xing, Y. Liu, Y. F. Gao and J. R. Liu, *Carbon*, 129 (2018) 819.
11. Y. Zhou, Y. L. Wang, J. F. Wang, L. Lin, X. Y. Wu and D. N. He, *Mater. Lett*., 216 (2018) 248.
12. F. Yang, K. B. Xu and J. Q. Hu, *J. Alloy Compud*., 729 (2017) 1172.
13. P. Wang, H. Zhou, C. F. Meng, Z. T. Wang, K. Akhtar and A. H. Yuan, *Chem. Eng. J*., 369 (2019) 57.
14. J. J. Qiu, Z. X. Bai, E. G. Dai, S. C. Liu and Y. Liu, *J. Alloy Compud*., 763 (2018) 966.
15. T. Dong, M. Li, P. Wang and P. Yang, *Int. J. Hydrogen Energy*, 43 (2018) 14569.
16. D. S. Patil, S. A. Pawar and J. C. Shin, *Chem. Eng. J*., 335 (2018) 693.
17. H. L. Zhu and Y. Q. Zheng, *Electrochim. Acta*, 265 (2018) 372.
18. L. J. Luo, T. M. Liu, S. Zhang, B. Ke, L. Yu, S. H. Hussain and L. Y. Lin, *Ceram. Int*., 43 (2017) 5095.
19. S. T. Li, Y. N. Duan, Y. Teng, N. Fan and Y. Q. Huo, *Appl. Surf. Sci*., 478 (2019) 247.
20. G. Lee and J. Jang, *J. Power Sources*, 423 (2019) 115.
21. H. Z. Wang, Z. Y. Guo, S. W. Yao, Z. X. Li and W. G. Zhang, *Int. J. Electrochem. Sci*., 12 (2017) 3721.
22. K. W. Qiu, Y. Lu, J. B. Cheng, H. L. Yan, X. Y. Hou, D. Y. Zhang, M. Lu, X. M. Liu and Y. S. Luo, *Electrochim. Acta*, 157 (2015) 62.
23. M. Cheng, S. B. Duan, H. S. Fan, X. R. Su, Y. M. Cui and R. M. Wang, *Chem. Eng. J*., 327 (2017) 100.